

AN ABSTRACT OF THE THESIS OF

Scott T. Griffiths for the degrees of Honors Baccalaureate of Science in Physics and Honors Baccalaureate of Science in Mathematics presented on June 4, 2008. Title: Seasonal and Solar Cycle Variations in High-Probability Reconnection Regions on the Dayside Magnetopause.

Abstract approved:

Henri Jansen

Future satellite missions like NASA's upcoming Magnetospheric Multiscale (MMS) mission are targeting reconnection diffusion regions at the Earth's magnetopause. These diffusion regions are small compared to the total surface area of the magnetopause. Furthermore, the location of the diffusion region depends on external parameters such as the current state of the Earth's magnetic field and the interplanetary magnetic field (IMF), which is frozen into the solar wind. Even given a complete set of these initial conditions, the location of the diffusion region is still the subject of ongoing research and has yielded several competing models.

Our objective is to locate areas on the magnetopause where the diffusion region may be found with a higher probability at a given time. Since the principal temporal variation in the Earth's magnetic field is governed by the Earth's seasonal dipole tilt and because solar conditions are roughly periodic over an eleven-year cycle, the external parameters on which the location of the diffusion region depends can be inferred from past data. Using this technique we will explore possible relationships between the terrestrial season and solar cycle and locations where the diffusion region may be found with higher probability. Several of the most popular reconnection models will be used in this analysis, including the tilted neutral line model of component reconnection, anti-parallel reconnection, and a hybrid scheme developed by the present authors which utilizes elements from each of these.

Key Words: anti-parallel, cusp, GSM coordinates, IMF, magnetic shear, magnetopause, magnetosphere, reconnection, solar cycle, subsolar point, T96

Corresponding E-mail Address: scott.griffiths@lifetime.oregonstate.edu

©Copyright by Scott T. Griffiths

June 4, 2008

All Rights Reserved

Seasonal and Solar Cycle Variations in High-Probability

Reconnection Regions on the Dayside Magnetopause

by

Scott T. Griffiths

A PROJECT

submitted to

Oregon State University

University Honors College

in partial fulfillment of
the requirements for the
degree of

Honors Baccalaureate of Science in Physics (Honors Scholar)
Honors Baccalaureate of Science in Mathematics (Honors Scholar)

Presented June 4, 2008
Commencement June 2008

Honors Baccalaureate of Science in Physics and Honors Baccalaureate of Science in Mathematics project of Scott T. Griffiths presented on June 4, 2008.

APPROVED:

Mentor, representing Physics

Committee Member, representing Physics

Committee Member, representing Physics

Chair, Department of Physics

Dean, University Honors College

I understand that my project will become part of the permanent collection of Oregon State University, University Honors College. My signature below authorizes release of my project to any reader upon request.

Scott T. Griffiths, Author

Table of Contents

	<u>Page</u>
1 Introduction.....	1
2 Methods	4
2.1 Simulating Magnetospheric Environmental Conditions.....	5
2.2 Predicting Magnetic Reconnection Line Locations.....	6
2.3 Calculating Reconnection Line Probability Distributions	9
2.4 Discussion of Sources of Error	11
3 Results.....	12
3.1 Seasonal Variations.....	12
3.1.1 Seasonal Variations Using the Tilted Neutral Line Model.....	13
3.1.2 Seasonal Variations Using the Anti-parallel Model	14
3.1.3 Seasonal Variations Using the Trattner Model.....	17
3.2 Solar Cycle Variations	21
3.2.1 Solar Cycle Variations Using the Tilted Neutral Line Model	22
3.2.2 Solar Cycle Variations Using the Anti-parallel Model.....	24
3.2.3 Solar Cycle Variations Using the Trattner Model	25
4 Conclusions.....	27
Bibliography	30
Glossary	31

List of Figures

<u>Figure</u>	<u>Page</u>
Figure 2.1 – The solar wind, incident from the right, is draped across the ellipsoidal magnetopause at the left. The magnetopause is colored according to the magnetic shear angle, which is the angle made between the IMF (shown) and the magnetopause magnetic field (partially shown).....	8
Figure 2.2 – Magnetic shear angle plots with reconnection lines overlaid. Shown at left is the anti-parallel reconnection line; at right is the maximum shear line used in the Trattner model.....	9
Figure 2.3 – Plot of ten reconnection lines added together	10
Figure 3.1 – Tilted neutral line seasonal reconnection line location probability distributions for 2005	13
Figure 3.2 – Example of the yearly variation in the seasonal probability distributions for the tilted neutral line model	14
Figure 3.3 – Anti-parallel seasonal reconnection line location probability distributions for 2005.....	16
Figure 3.4 – Example anti-parallel line for an IMF with a large negative B_z component	17
Figure 3.5– Trattner model seasonal reconnection line location probability distributions for 2005.....	18
Figure 3.6 – Sunspot Cycle 23. Image from NorthWest Research Associates, Inc.	21
Figure 3.7 – Comparison of probability distributions at solar maximum (left) and near solar minimum (right) using the tilted neutral line model	22
Figure 3.8 – ACE solar wind data for October 2001 showing IMF B_x , B_y , and B_z components as well as the IMF clock angle	23
Figure 3.9 – ACE solar wind data for October 2005 showing IMF B_x , B_y , and B_z components as well as the IMF clock angle	24
Figure 3.10 – Comparison of probability distributions at solar maximum (left) and near solar minimum (right) using the anti-parallel reconnection line model	25
Figure 3.11 – Comparison of probability distributions at solar maximum (left) and near solar minimum (right) using the Trattner model	26

1 Introduction

Magnetic reconnection is a ubiquitous and powerful force in the astrophysical setting. Reconnection is thought to be the driving force behind many astrophysical phenomena, including solar flares and plasma advection in the Earth's magnetosphere. Although reconnection can be observed in a laboratory setting, the highly-energetic plasmas generated by astrophysical sources like the Sun makes space an ideal setting to make *in situ* observations of reconnection as it occurs. However, making observations using spacecraft is a costly and difficult endeavor, and it requires a significant amount of careful planning.

Future spacecraft missions are currently being planned to investigate the physics that occurs at reconnection diffusion regions, which are the locations where magnetic field lines merge before peeling away under the general convection of the solar wind. One such mission is NASA's Magnetospheric Multiscale (MMS) satellite cluster, which is currently scheduled for launch in 2015. Using solar wind conditions measured over a solar cycle, the conditions that the MMS mission is likely to encounter as a function of solar cycle and season can be estimated. Furthermore, when these data are used in conjunction with an appropriate model of where reconnection can occur as a function of solar wind and magnetospheric conditions, the location of the reconnection site can be estimated for each season and over a solar cycle. These estimates, combined with orbit predictions for the MMS spacecraft, can then provide estimates of the probabilities of encountering the reconnection diffusion region over the life of the mission.

In this paper we discuss a computational method for generating these probabilities and present a statistical study of reconnection site location as a function of season and solar cycle. Our results are generated using solar wind data from 2001 to 2006, which represents a half solar cycle from solar maximum to solar minimum. Magnetospheric conditions are simulated using the T96 model [Tsyganenko, 1995], which generates a realistic magnetopause based on the incoming IMF and solar wind dynamic pressure. These are then combined with a selection of models which can predict where reconnection is likely to occur on the dayside magnetopause based on the solar wind IMF and the magnetospheric conditions it induces, including the tilted neutral line model, the anti-parallel model, and the Trattner model.

The reconnection models used in this paper represent the most commonly accepted and widely used reconnection site location theories. All of these models predict that reconnection diffusion regions are spread out along long, thin lines, which is in good agreement with the current body of experimental evidence [Phan *et al.*, 2006]. Reconnection was originally thought to occur only where the IMF is aligned anti-parallel to the Earth's magnetic field because of efficiency arguments, as outlined by Dungey [1961], but observational data indicates that this need not be the case. As an alternative, component reconnection models were developed, such as the tilted neutral line model [Sonnerup, 1970; Moore *et al.*, 2002] and the recently proposed Trattner model [Trattner *et al.*, 2007]. The Trattner model represents the state of the art and has been shown to have excellent agreement with observations.

These tools are then used to search for patterns and trends in the distribution of reconnection line locations based on season and solar cycle. Although the Trattner model

is thought to provide the most accurate predictions of reconnection line locations, each of the three models is included in our analysis for comparison. By determining the impact of seasonal and solar cycle variations on reconnection line distributions, the conditions that spacecraft like MMS are likely to encounter as a function of solar cycle and season can then be estimated.

2 Methods

The magnetosphere represents a complex environment that is difficult and costly to directly observe. Computer-based simulations offer an attractive option to generate predictions which can be tested by in situ measurements and to analyze and interpret currently available data. This study relies on a computational simulation which was designed to predict where reconnection is likely to take place across the magnetopause given a particular set of IMF and magnetospheric environmental parameters. Although MHD computations are often employed for reconnection calculations, running MHD simulations is computationally expensive and is overkill for the purposes of this study, which seeks only to determine a relative probability of locating a reconnection event at a particular location.

We instead chose to create our own end-to-end simulation by combining several popular theoretical models. Our simulation can be partitioned by function into three distinct parts: setting up a model magnetosphere from a given set of solar wind conditions, modeling the interaction of the solar wind with our virtual magnetosphere and predicting where reconnection is likely to occur on the magnetopause (it has been shown that reconnection is always occurring somewhere on the magnetopause), and compiling all of the predicted reconnection lines over a period of time to create a probability map of where reconnection is most likely to occur during that time period.

The remainder of this section will be devoted to a discussion of the three main parts of our code, estimates of the total error expected to accumulate throughout the code, and an explanation of how to interpret our data.

2.1 Simulating Magnetospheric Environmental Conditions

The first section of our code uses solar wind data from the Advanced Composition Explorer (ACE) satellite and models the magnetic field at the magnetopause using the T96 model [Tsyganenko, 1995]. The data that we used from ACE included IMF direction and magnitude as well as solar wind density and velocity, which were needed to compute the dynamic pressure ($p_{\text{dyn}} = \frac{1}{2}\rho v^2$). We had nearly six years worth of solar wind data available, from mid-2001 to the end of 2006, with data points every three minutes. This time span represents a half solar cycle, extending from solar maximum in late 2001 to near solar minimum at the end of 2006. It should be noted that although the solar wind is sampled by ACE at the L1 Lagrange point, we made the simplifying assumption that solar wind conditions would be the same at the magnetopause since solar wind conditions change very little over this short distance (about 1% of the distance from the Sun to the Earth). This simplification does not represent a significant source of error, as will be discussed later in this section.

The magnetospheric magnetic field, which is generated by the Earth's internal dynamo, was simulated using Tsyganenko's popular T96 model. This model confines the Earth's magnetic field within an ellipsoidal magnetopause whose size varies according to the dynamic pressure exerted by the solar wind. The T96 model also takes into account the Y_{GSM} and Z_{GSM} components of the solar wind and the dipole tilt of the Earth. With the size and shape of the magnetopause known, we then drape the solar wind's frozen-in IMF across the magnetopause and compute the magnetic shear angle – which is simply the angle between the draped IMF and the magnetopause magnetic field vectors – at each point on the surface of the magnetopause.

2.2 Predicting Magnetic Reconnection Line Locations

The second section of our code uses a selection of popular theoretical models which predict where a reconnection x-line is likely to occur across the magnetopause based on the magnetic shear. At present, reconnection is not yet completely understood and there are many questions regarding the necessary and optimal conditions for reconnection to occur. Most of the theories which attempt to predict the location of reconnection x-lines are based primarily on satellite observations. Unfortunately, reconnection is very difficult to observe as it occurs, and as a result reconnection theories have evolved in time as the available data set has improved in quantity and quality.

One of the earliest and most successful reconnection theories was originally developed by *Dungey* [1961]. According to this theory, which is generally referred to as anti-parallel reconnection, reconnection is most likely to occur where the magnetic shear angle is nearly 180° . As discussed by *Crooker* [1979], the anti-parallel model predicts that a reconnection x-line is most likely to form where the magnetic shear is within $\pm 30^\circ$ of anti-parallel. This leads to some interesting reconnection line topologies, including an x-line which bifurcates at the noon meridian when the IMF is southward (negative z in GSM coordinates). In particular, the anti-parallel model predicts that reconnection is almost always occurring near the magnetospheric cusps.

However, space craft observations have shown that reconnection often occurs in regions where the magnetic shear is far from anti-parallel, particularly near the subsolar point. These observations are often explained by component reconnection theories, so called because they assert that the IMF and magnetospheric magnetic field need only to have components which are anti-parallel rather than having exactly opposite polarity.

One of the more popular component reconnection theories is the tilted neutral line model [Sonnerup, 1970], which predicts that reconnection occurs along a line extending from the subsolar point in a direction governed by the IMF clock angle. Notably, this theory predicts that reconnection occurs continuously at the subsolar point, which is not what is observed. As a result, this theory has largely fallen out of use in its original form, although several modified versions of it are still popular.

A recent model proposed by *Trattner* [2007] contains parts of both the anti-parallel and component reconnection theories. Depending on IMF conditions, the Trattner model predicts that the actual reconnection line position is given by either the anti-parallel model or a combination anti-parallel and component x-line. Specifically, in the cases where the IMF very nearly due south (within 30°) or when the X_{GSM} component of the IMF is large (greater than 70% of the total IMF magnitude), the Trattner model defaults to anti-parallel reconnection. In all other cases, the Trattner model predicts that the reconnection line will be mostly anti-parallel except near the subsolar point, where a tilted x-line joins the bifurcated anti-parallel regions. One feature of the Trattner model that distinguishes it from the other two reconnection line theories is that the Trattner model accounts for the dipole tilt of the Earth by allowing the center of the tilted x-line that joins the anti-parallel regions to float northward or southward of the subsolar point based on where the magnetic shear is greatest. This contrasts sharply with the standard titled neutral line component model, which predicts that reconnection always occurs at the subsolar point, and the anti-parallel model, which predicts that reconnection at or near the subsolar point only occurs for strongly southward IMF conditions.

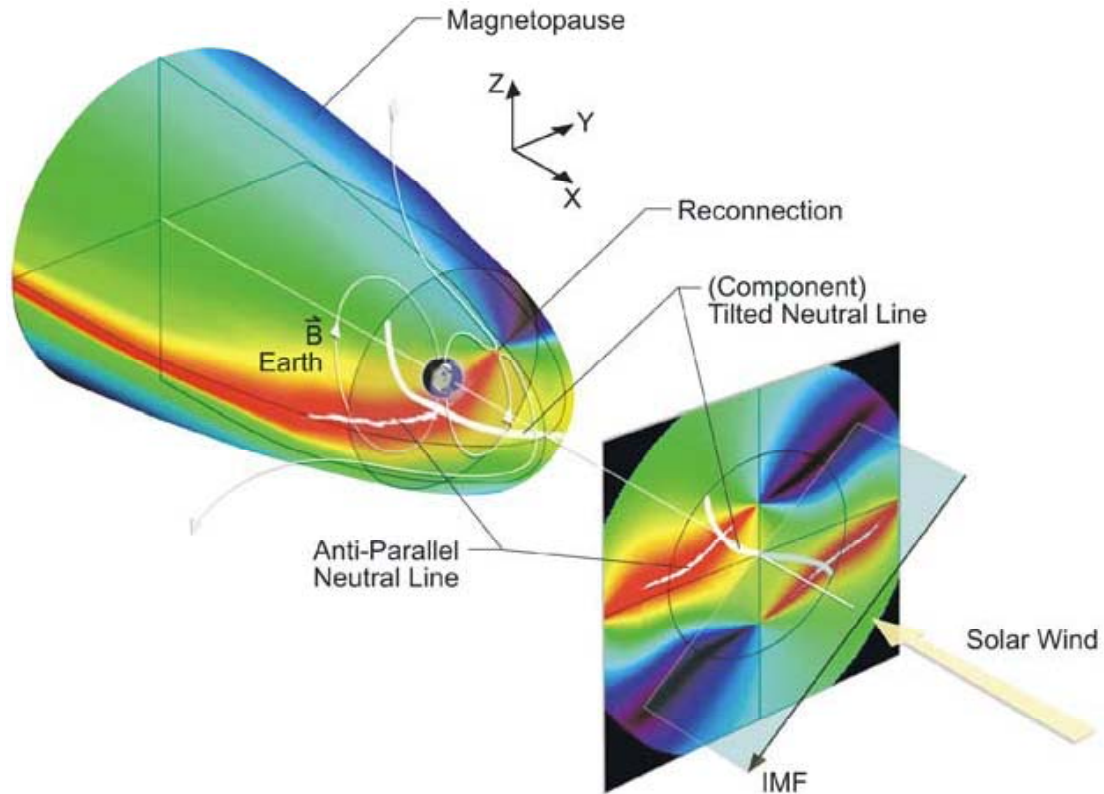


Figure 2.1 – The solar wind, incident from the right, is draped across the ellipsoidal magnetopause at the left. The magnetopause is colored according to the magnetic shear angle, which is the angle made between the IMF (shown) and the magnetopause magnetic field (partially shown). The result is then projected onto the Y-Z GSM plane. Note the white reconnection lines and the terminator plane, which separates the day side from the night side. Image courtesy from [Trattner et al., 2007].

In practice, the reconnection lines are computed using the magnetic shear angles from the first part of the code. The exception is the simple tilted neutral line, which is simply a line which is at an angle to the Y_{GSM} axis of the IMF clock angle divided by two. Although we have included the tilted neutral line in our discussions because of its historical popularity, very little analysis was done using this antiquated model. The anti-parallel reconnection line is computed by first finding the Z_{GSM} location of the maximum shears at $\pm 20 R_E$ (Earth radii) along the Y_{GSM} axis. Once the maximum shears are found at the left and right boundaries, one simply walks along the path of maximum shear

towards the noon meridian ($Y_{\text{GSM}} = 0$). To compute the combined anti-parallel and component line for the Trattner model, which we call the maximum shear line, we simply compute the maximum shear within $\pm 0.1 R_E$ of the Y_{GSM} axis and then walk along a line of maximum shear until we connect with the two anti-parallel lines. Of course, there are quite a few technical difficulties in implementing these algorithms, but the basic ideas are straightforward. The different types of reconnection lines can be seen below.

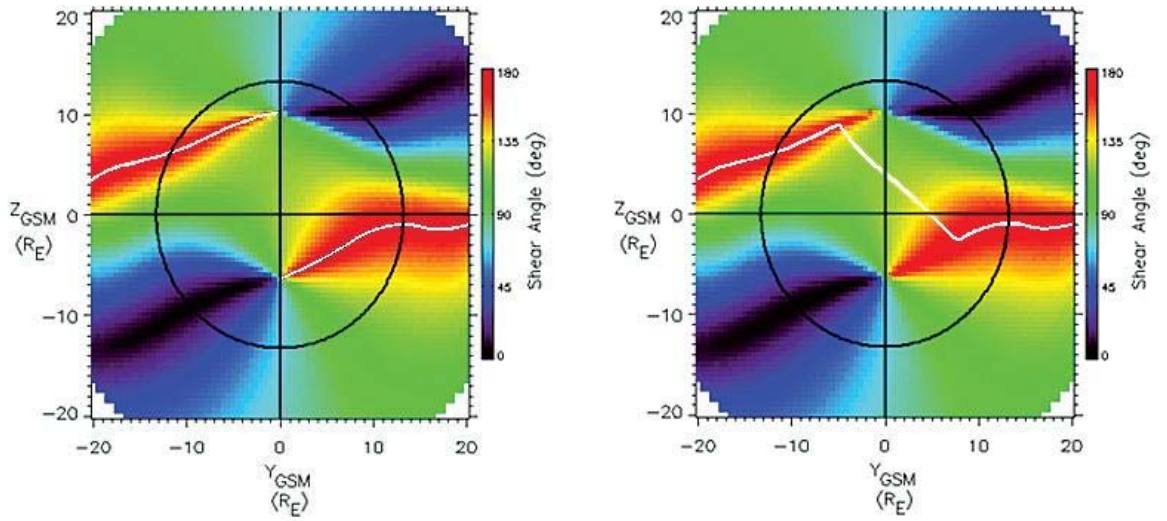


Figure 2.2 – Magnetic shear angle plots with reconnection lines overlaid. Shown at left is the anti-parallel reconnection line; at right is the maximum shear line used in the Trattner model. Both reconnection lines are shown in white. The black circle represents the location of the terminator plane.

2.3 Calculating Reconnection Line Probability Distributions

The third and final section of our code takes the reconnection lines generated in the previous section and translates them into probability maps. As was briefly mentioned before, the solar wind data from ACE are separated by three minute intervals. At each time interval, the ACE data is fed into the first two sections of the code and three reconnection lines are generated, one for each of the three reconnection line models.

Each set of reconnection lines is then summed over a given time interval (we used monthly and seasonal time periods) and divided by the number ACE data points within the time period to create a probability map of where reconnection is most likely to occur on the magnetopause.

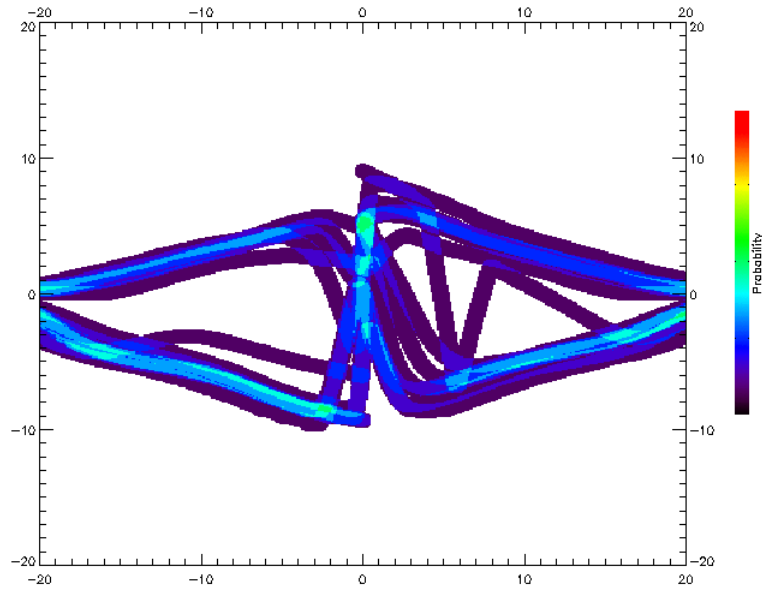


Figure 2.3 – Plot of ten reconnection lines added together. The probability of at any given point is given by the number of reconnection lines passing through that point divided by the total number of reconnection lines.

Reconnection lines are believed to be very long and thin, as discussed by *Phan et al.* [2006], so in order to sum the reconnection lines in a meaningful way we first widen them to a width of $1 R_E$ (each point along the reconnection line is expanded to a disk of radius $0.5 R_E$). The reason behind the choice of this diameter is twofold. As will be discussed in the next section of this paper, the total error accumulated throughout this code is estimated to be approximately $1 R_E$, so widening the reconnection line to this diameter builds in this uncertainty. Second, in order for a space craft to make precise measurements of reconnection as it occurs it is estimated that the craft must be within 0.5

R_E of the reconnection x-line, so assuming that there is no error in our results, the widened reconnection lines yield the regions where a space craft would be able to take good measurements.

2.4 Discussion of Sources of Error

It is exceedingly difficult to estimate the error from a large research code like the one used to create the data for this paper, which is roughly 7,500 lines long. However, we will attempt to enumerate some possible sources of error and put an upper bound on the amount of error these sources could introduce.

The most obvious place where errors could be significant is in modeling the magnetospheric magnetic field. As we have said, the magnetosphere is a very complex system; how do we know if we are modeling it accurately? This is a very difficult question to answer. In fact, no rigorous testing of the T96 model has ever been done, even though it is one of the most frequently used data-based models of the Earth's magnetic field. However, *Trattner et al.* [2007] has a detailed explanation of the possible sources of error from the T96 model and puts an upper bound of $1 R_E$ on the total error.

The other obvious source of error in the code comes from the reconnection line models. These models are purely theoretical and have not been proven rigorously; indeed, one of the purposes of the research done for this paper is to aid in the planning of the next generation of satellites, whose data will be invaluable in refining these models. The reconnection line models used for this paper (particularly the Trattner model) have been checked as thoroughly as possible against the best data currently available, and that is the best that can be done. Thus the total error in our code is a matter of speculation.

3 Results

The purpose of this study is to look for seasonal and solar cycle-based trends in the reconnection line location probability distributions using all three reconnection line theories (tilted neutral line, anti-parallel, and the Trattner model). The analyses were conducted by examining the probability distributions generated by our code.

3.1 Seasonal Variations

We first looked at how the reconnection line location probability distributions (hereafter called probability distributions) varied according to season. For the purposes of this paper, we define a season to be a three month interval roughly corresponding to the normal seasons experienced in the Northern hemisphere. Our grouping of the months into four seasons is given in the table below:

Spring	Summer	Fall	Winter
February	May	August	November
March	June	September	December
April	July	October	January

Aside from the normal variations in the IMF due to the complex dynamics of the sun's magnetic field, we expect that there should be definite variations in the probability distributions due to the seasonal dipole tilt of the Earth since the dipole tilt will change the orientation of the magnetopause with respect to the Sun. We also anticipate that the probability distributions for each season will vary little from year to year since fluctuations in the IMF should be averaged out over the large time period of a whole season.

3.1.1 Seasonal Variations Using the Tilted Neutral Line Model

We will first discuss seasonal variations in the reconnection line probability distribution using the tilted neutral line model. As we discussed in the methods section of this paper, the tilted neutral line model is extremely simple: the angle of the tilted neutral line depends only on the IMF clock angle and does not take changing magnetospheric conditions into account. As a result, we expect that we will not see any variations in the probability distributions based on the Earth's dipole tilt. However, because of the Parker spiral structure of the solar wind, we expect that the distribution of solar wind sectors should yield obvious differences between the different seasons.

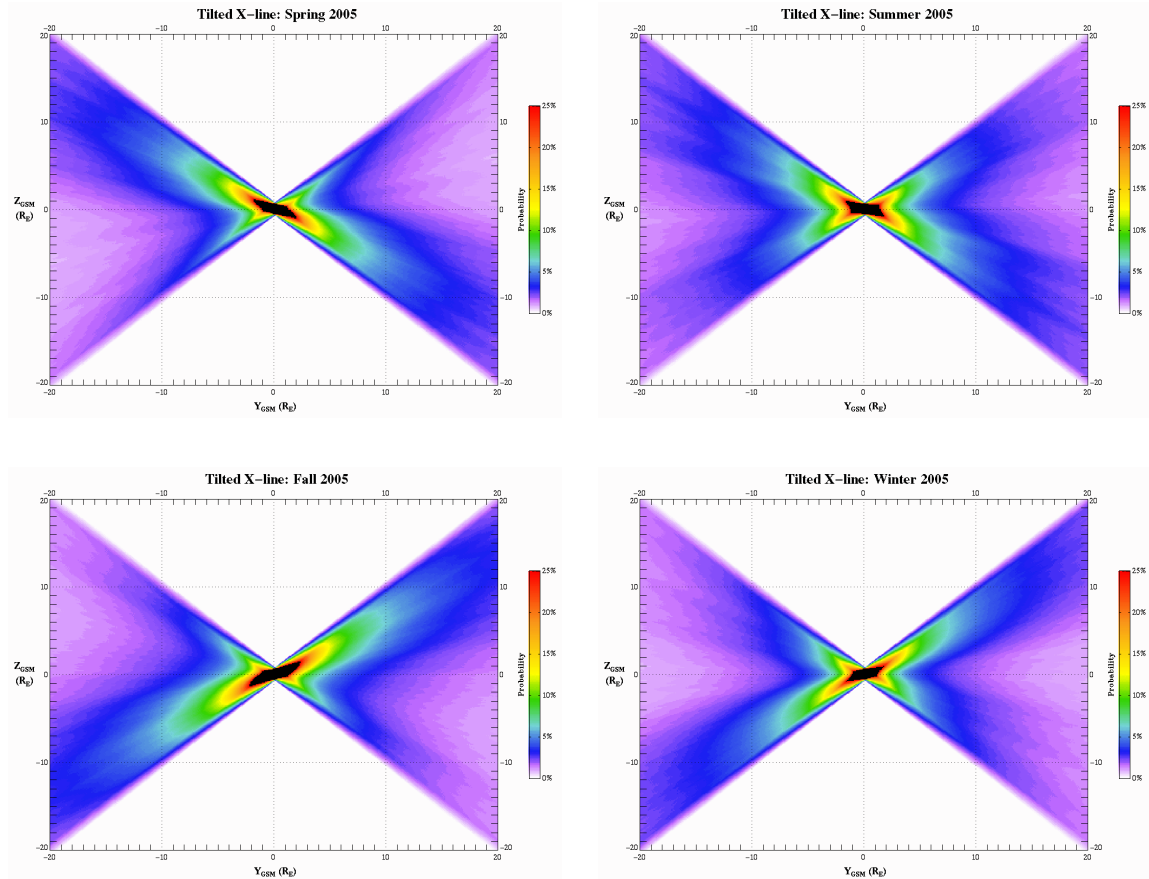


Figure 3.1 – Tilted neutral line seasonal reconnection line location probability distributions for 2005. (Upper Left): Spring 2005. (Upper Right): Summer 2005. (Lower Left): Fall 2005. (Lower Right): Winter 2005

We note that spring and fall appear to be opposite of each other, each one favoring a particular IMF clock angle orientation. In contrast, the summer and winter seasons appear to be more balanced. While these plots don't accurately reflect reconnection line locations, they do give us a clear indication of how the average IMF clock angle varies by season. Furthermore, the average IMF clock angle for a particular season appears to vary little from year to year, as evidenced by the plots below.

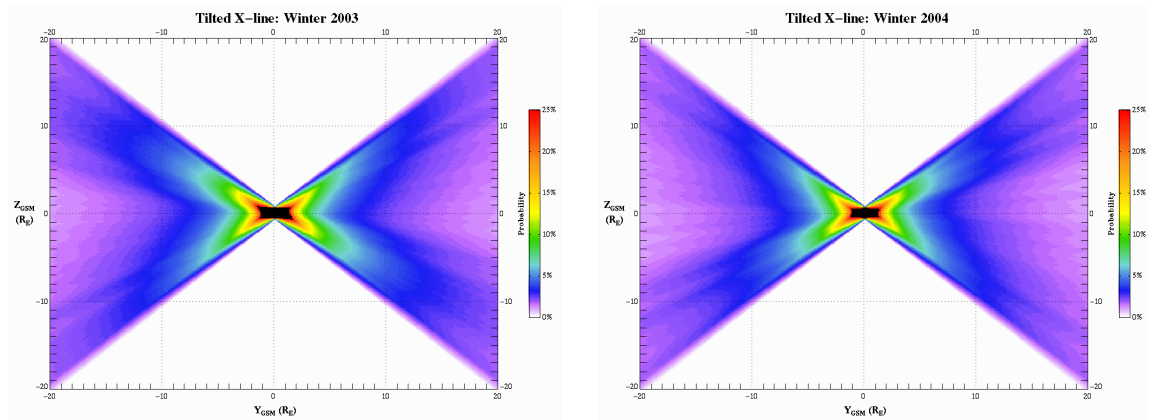


Figure 3.2 – Example of the yearly variation in the seasonal probability distributions for the tilted neutral line model. (Left): Winter 2003. (Right): Winter 2004.

3.1.2 Seasonal Variations Using the Anti-parallel Model

In contrast to the tilted neutral line model, the anti-parallel model does take magnetospheric conditions into account. As a result, we expect to see a strong seasonal dependence in our anti-parallel data, which is what is observed in the figures below. We observe two distinct processes at work: the effect of the Earth's dipole tilt, and the effect of the correlation between solar sectors and season that was observed in the tilted neutral line case.

In the spring and the fall, we see that the cusps (seen in the figures as yellow or red spots) are located at roughly $10 R_E$ above and below the Earth, indicating that the Z_{GSM} axis (which is aligned with the Earth's dipole tilt) is perpendicular to the Earth-Sun line (the X_{GSM} axis). This causes the reconnection line distributions to be approximately symmetric about the $Z_{GSM} = 0$ axis. However, we also see the same effects of the IMF clock angle distribution as we saw from looking at the tilted neutral line model. This causes the reconnection lines to tend towards the northern cusp for negative Y_{GSM} and towards the southern cusp for positive Y_{GSM} during the spring, while in the fall the opposite occurs.

The summer and winter seasons show quite the opposite behavior. In the summer season the cusps are shifted down by about $2 R_E$, and in the winter they are shifted upwards by the same amount. This causes more the reconnection lines to appear more frequently to the south in the summer and more frequently to the north in the winter. However, as we saw in the tilted neutral line case, the solar sectors during these seasons cause the IMF clock angles to be distributed approximately evenly, so in the summer and winter the probability distributions are approximately symmetric about the $Y_{GSM} = 0$ axis.

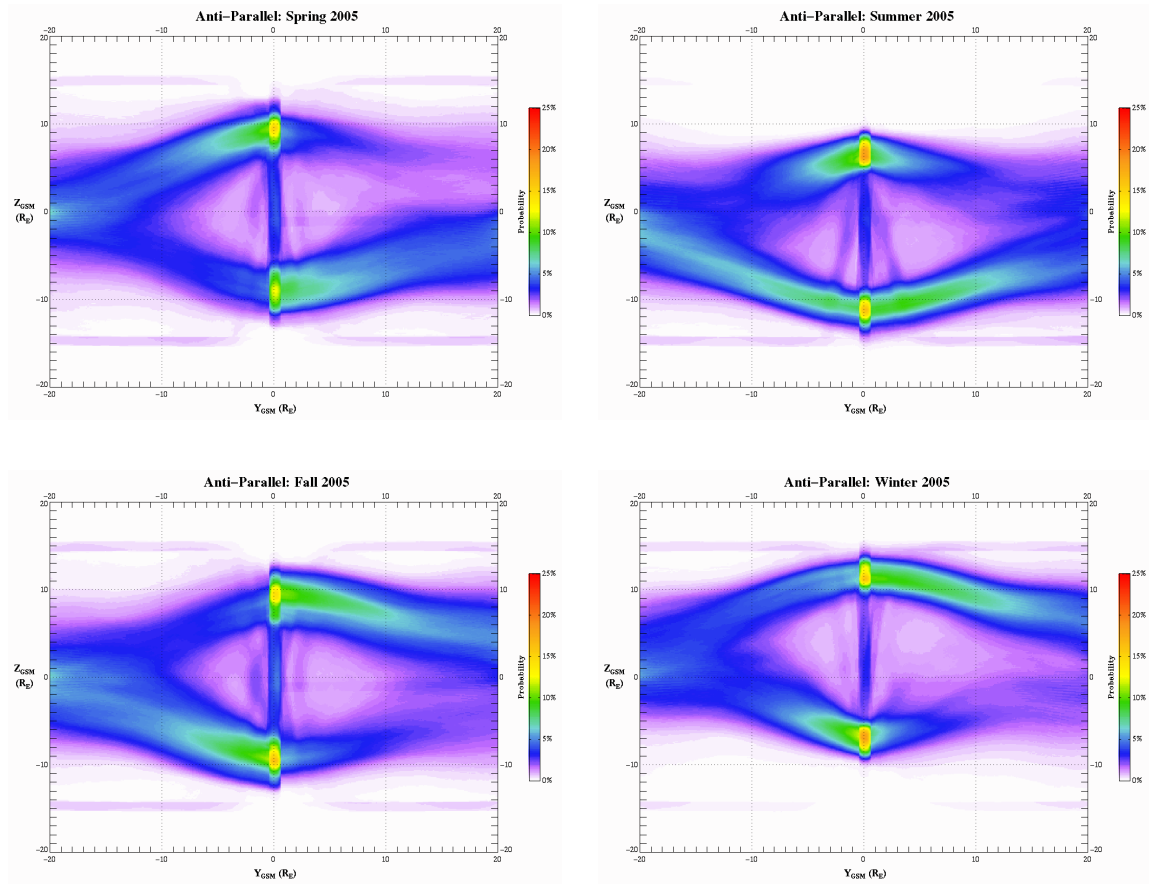


Figure 3.3 – Anti-parallel seasonal reconnection line location probability distributions for 2005. (Upper Left): Spring 2005. (Upper Right): Summer 2005. (Lower Left): Fall 2005. (Lower Right): Winter 2005.

Some comments are in order regarding some technical details that can be observed in the above plots. First, note the purple horizontal lines that appear at $Z_{\text{GSM}} = \pm 15 R_E$. These lines are not physical; they are actually an artifact of the code, which restricts the reconnection lines to this region. This is done because the terminator is at $15 R_E$, which means that beyond this point you enter the magnetotail region, which is beyond the scope of this study.

Second, note that the right sides ($Y_{\text{GSM}} = 20 R_E$) of the plots in Figure 3.3 seem to be thicker than on the left sides ($Y_{\text{GSM}} = -20 R_E$). We are uncertain as to the exact origin

of this phenomenon, but it seems likely that it could be the result of how the IMF is draped onto our model magnetopause. A new draping method is currently being developed and will allow us to test this prediction.

Finally, note the blue vertical line that appears along the $Y_{\text{GSM}} = 0$ axis in all of the figures. This line was determined to be the result of anti-parallel lines which have a single sinusoidal-like oscillation, like in Figure 3.4 below.

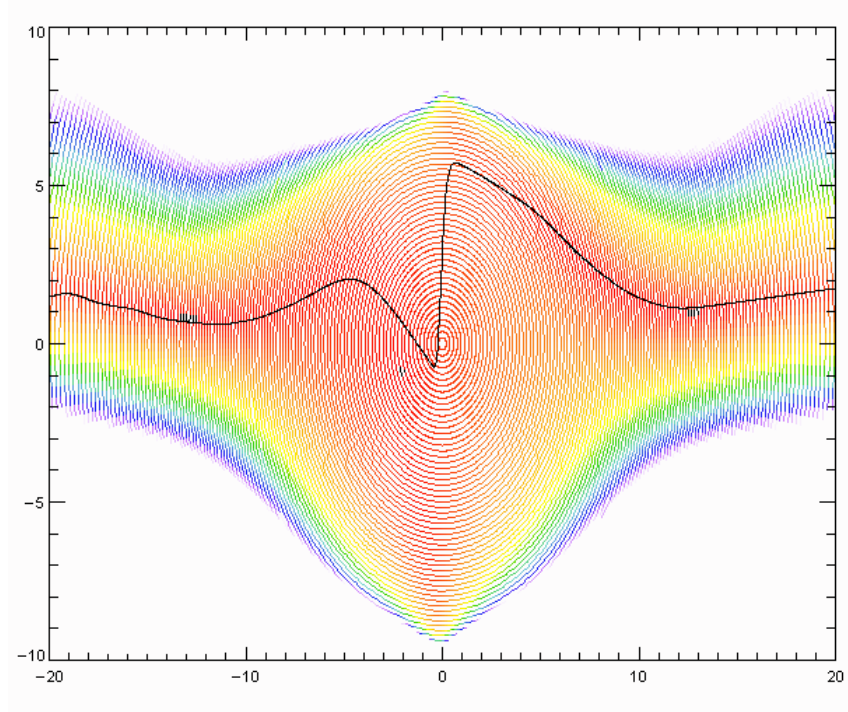


Figure 3.4 – Example anti-parallel line for an IMF with a large negative B_z component. Colored lines depict the magnetic shear angle on a rainbow scale, with red indicating anti-parallel field conditions.

3.1.3 Seasonal Variations Using the Trattner Model

As noted in the methods section, the Trattner model utilizes both anti-parallel reconnection lines and maximum shear reconnection lines, depending on IMF conditions. The computation of both reconnection lines depends heavily on magnetospheric conditions, so we again expect that there should be a strong seasonal dependence.

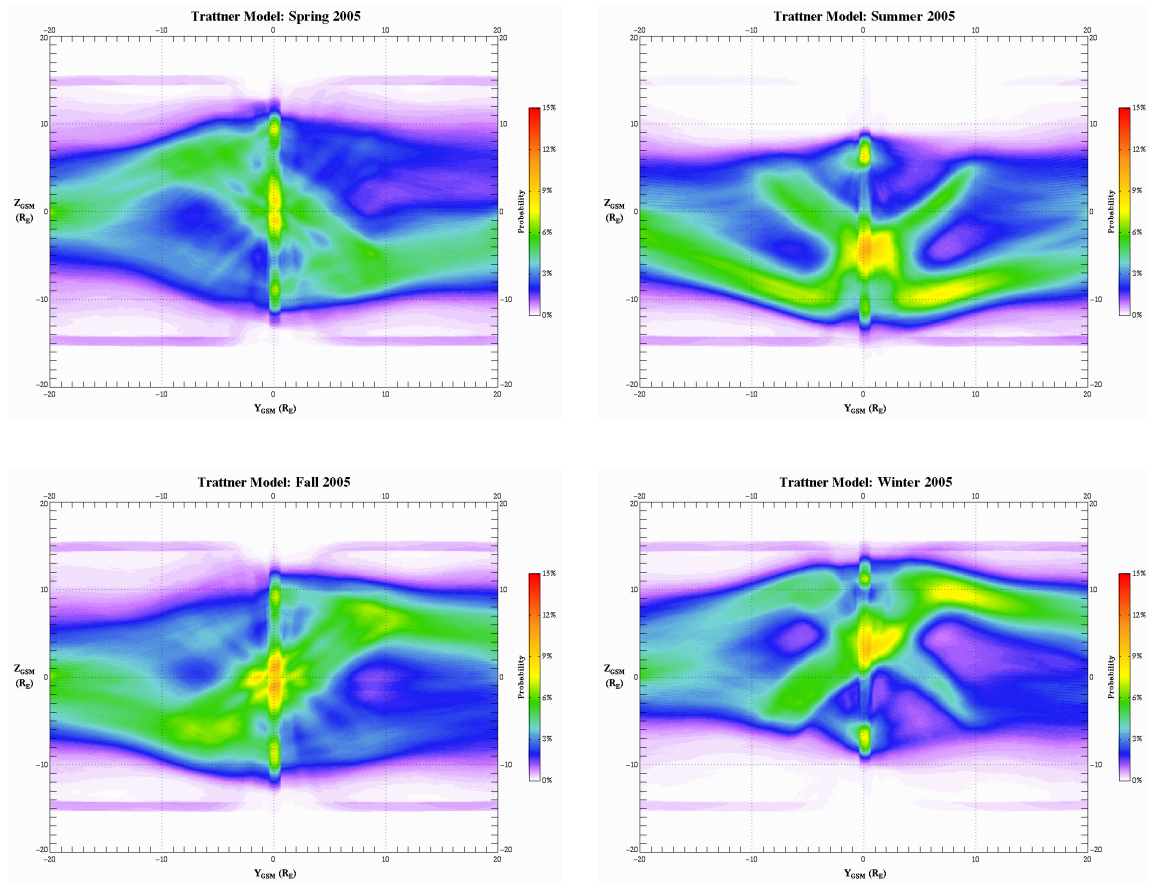


Figure 3.5— Trattner model seasonal reconnection line location probability distributions for 2005. (Upper Left): Spring 2005. (Upper Right): Summer 2005. (Lower Left): Fall 2005. (Lower Right): Winter 2005.

From Figure 3.5, we see that the maximum shear line plays the dominant role in determining the probability distribution for the Trattner model, as evidenced by the thick green diagonal regions near the subsolar point ($Y_{\text{GSM}} = Z_{\text{GSM}} = 0$). However, we recall from the methods section and from Figure 2.2 that the maximum shear line merges with the reconnection line, usually near $Y_{\text{GSM}} = \pm 10 R_E$. Therefore we expect that the probability distributions should be essentially the same in these regions as the distributions in Figure 3.4. At a glance it would appear that this is not the case, but it is important to note that different coloring scales are being used: the probability range for

the strictly anti-parallel plots in Figure 3.4 goes from 0 – 25%, while the Trattner model plots in Figure 3.5 use a probability range of 0 – 15%. The reason behind this switch is that the Trattner model probability distributions are spread more evenly across the Y-Z GSM plane than the anti-parallel distributions. After correcting for the scale difference, it is easy to see that the anti-parallel model and the Trattner model are indeed identical in this region. However, the two models yield distinctly different results within the terminator (the day side region), which is the region we are primarily interested in.

One of the most interesting results of the Trattner model is that there is a high-probability region at or near the subsolar point, just like the venerated tilted neutral line model. In fact, the Trattner model predicts that reconnection can be observed with the highest probability at the subsolar point about 50% of the time, during the spring and fall seasons. It is easy to see how observations made during these times at the dayside magnetopause would lead to the tilted neutral line theory. In contrast to the tilted neutral line theory, however, the Trattner model predicts that the high-probability region near the subsolar point should shift up or down with the Earth's dipole tilt by a sizeable amount ($\pm 4 R_E$). One obvious consequence of this is that a space craft that is sent to the subsolar point in May to observe reconnection will have a much lower probability of being close to a reconnection line than would be predicted by the tilted neutral line model, which predicts that reconnection should be occurring at the subsolar point continuously. However, if by looking at the Trattner model predictions you instead sent your space craft $4 R_E$ down the magnetopause from the subsolar point, you would triple your chances of being close to a reconnection line.

The Trattner model also makes some predictions which are quite different than the anti-parallel model. Looking at Figure 3.4 we note that to the left and right of the subsolar point there are fairly large regions where there is a very low probability of finding a reconnection line (no more than 3%). However, the Trattner model predicts that the probability of observing a reconnection line passing through these same regions should be approximately double the probability predicted by the anti-parallel model during all four seasons. This is an important result because in practice it is often easiest to put a satellite in an orbit which lies in the ecliptic plane (the $Y_{\text{GSM}} = 0$ plane). The Trattner model also predicts that there should be a high probability of observing a reconnection line near the cusps, which is in agreement with the anti-parallel theory, but the Trattner model predicts that this occurs about half as frequently as the anti-parallel model says it should.

In summary, the Trattner model has a strong seasonal dependence which yields some very different predictions than either of the two older reconnection line models. In particular, the Trattner model predicts that reconnection lines occur with the highest probability in a region near the subsolar point that shifts up and down with the Earth's dipole tilt and near the cusps. However, the Trattner model also predicts a reconnection line probability distribution that is much more evenly distributed across the magnetopause than either of the other two reconnection line models. Therefore, according to the Trattner model it seems that attempting to optimize a space craft orbit to maximize the probability of passing close to a reconnection line based on seasonal effects may yield smaller gains than would be possible if using the anti-parallel or tilted neutral line models.

3.2 Solar Cycle Variations

In addition to seasonal variations, we also looked for trends in the distributions of reconnection lines due to variations in solar activity. It is well known that solar activity proceeds through a 22 year cycle; however, it is common to speak of an 11 year sunspot cycle (i.e., to ignore polarization effects), in which the number of sunspots follows a sinusoidal-like distribution. The sunspot cycle of interest in this paper is Cycle 23, as seen below in Figure 3.6.

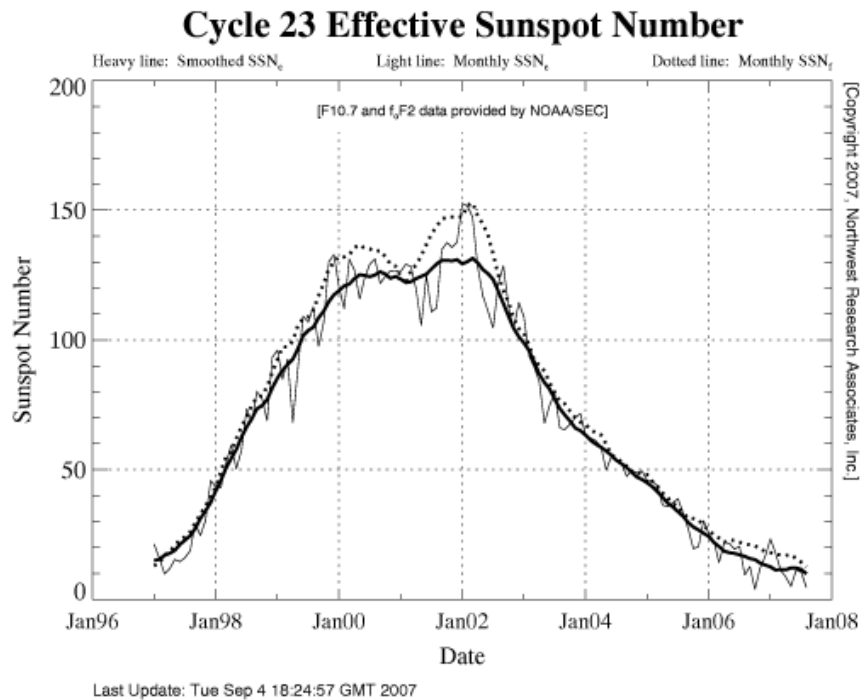


Figure 3.6 – Sunspot Cycle 23. Image from NorthWest Research Associates, Inc.
<http://www.nwra-az.com/spawx/ssne-cycle23.html>

In particular, we are interested in differences in reconnection line distributions between solar maximum (2001-2002) and solar minimum (we used data from 2006 since we did not have more recent data available). We will look for any patterns that may appear as a result of solar cycle differences using each of our three reconnection line models.

3.2.1 Solar Cycle Variations Using the Tilted Neutral Line Model

We compare both monthly and seasonal distributions for the tilted neutral line model in Figure 3.7 below. Looking at these plots, the tilted neutral line plots at solar minimum and solar maximum appear to be identical to a very high degree. The implication of this result is that the distribution of solar wind clock angles is essentially the same at solar maximum as they are at solar minimum, which is a rather unexpected result since the Sun's magnetic field at solar maximum is completely different than at solar minimum.

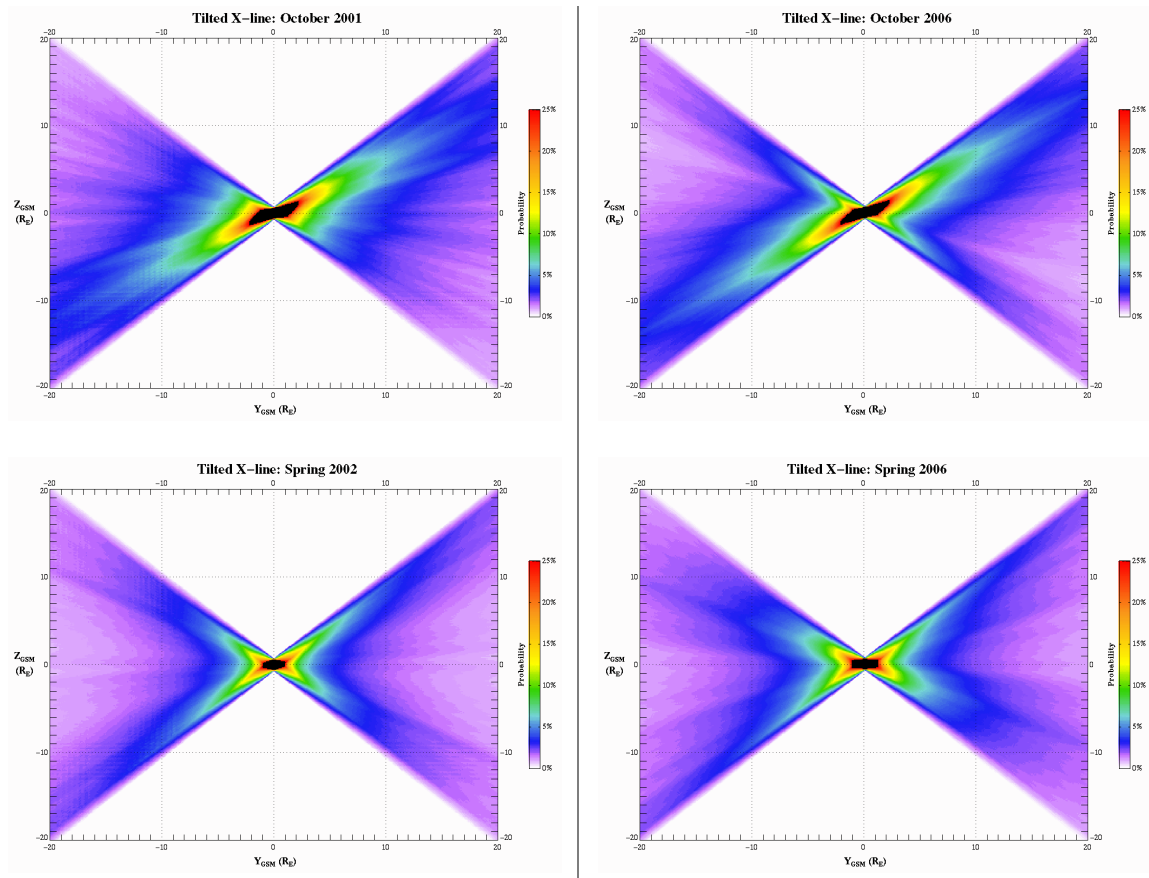


Figure 3.7 – Comparison of probability distributions at solar maximum (left) and near solar minimum (right) using the tilted neutral line model. The top two plots show probability distributions for the month of October, while the bottom plots show the probability distributions for spring of 2002 and 2006.

Looking at the raw ACE data for October 2001 (Figure 3.8) and October 2005 (Figure 3.9), we see that the solar wind is actually quite different at solar maximum than it is at solar minimum. At solar maximum (October 2001), the IMF appears to be fluctuating in a random manner. However, near solar minimum (October 2005), we see that the solar wind changes approximately weekly in a fairly regular pattern. This is most apparent when looking at the smoothed blue lines for the IMF B_x component and the clock angle. It is important to note that while Figure 3.7 implies that the clock angle distributions are roughly the same at solar minimum and solar maximum, it does not tell us anything about how the magnitude of the IMF changes. We will discuss this further in the following sections.

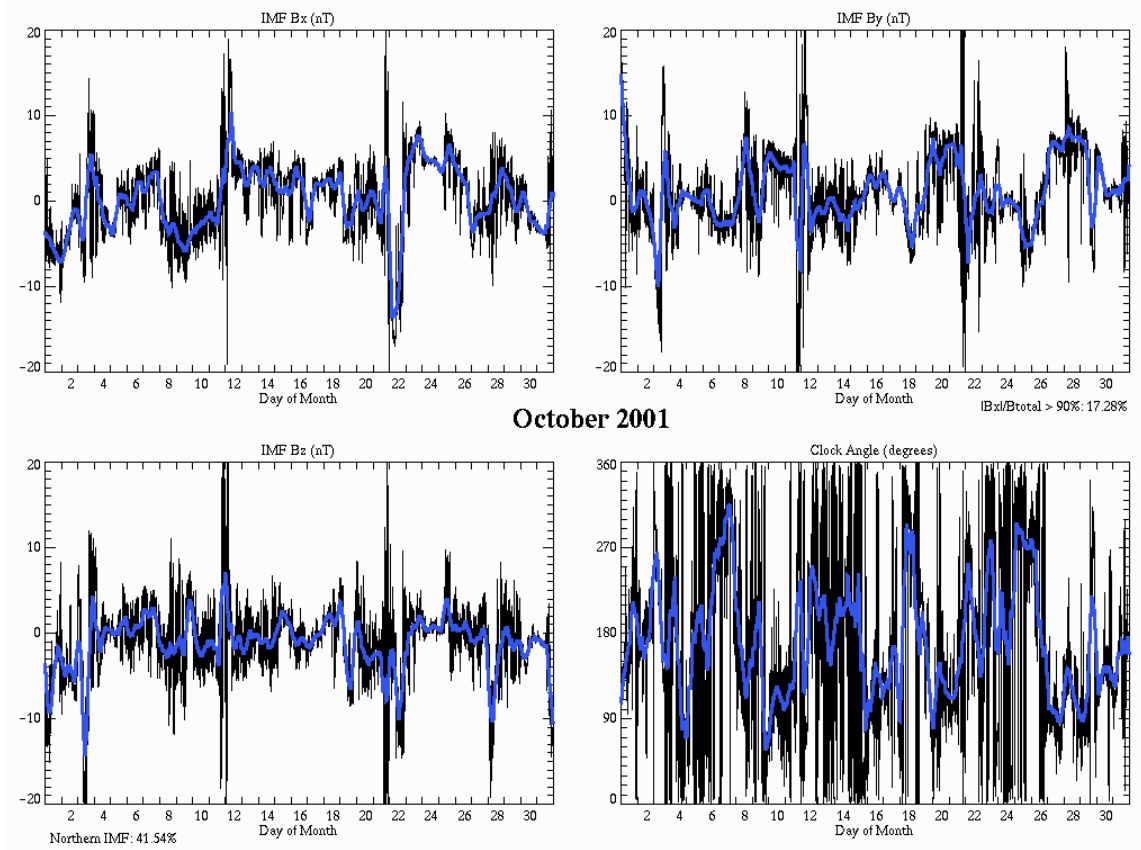


Figure 3.8 – ACE solar wind data for October 2001 showing IMF B_x , B_y , and B_z components as well as the IMF clock angle. The overlaid blue line shows a smoothed version of the data as a visual aid.

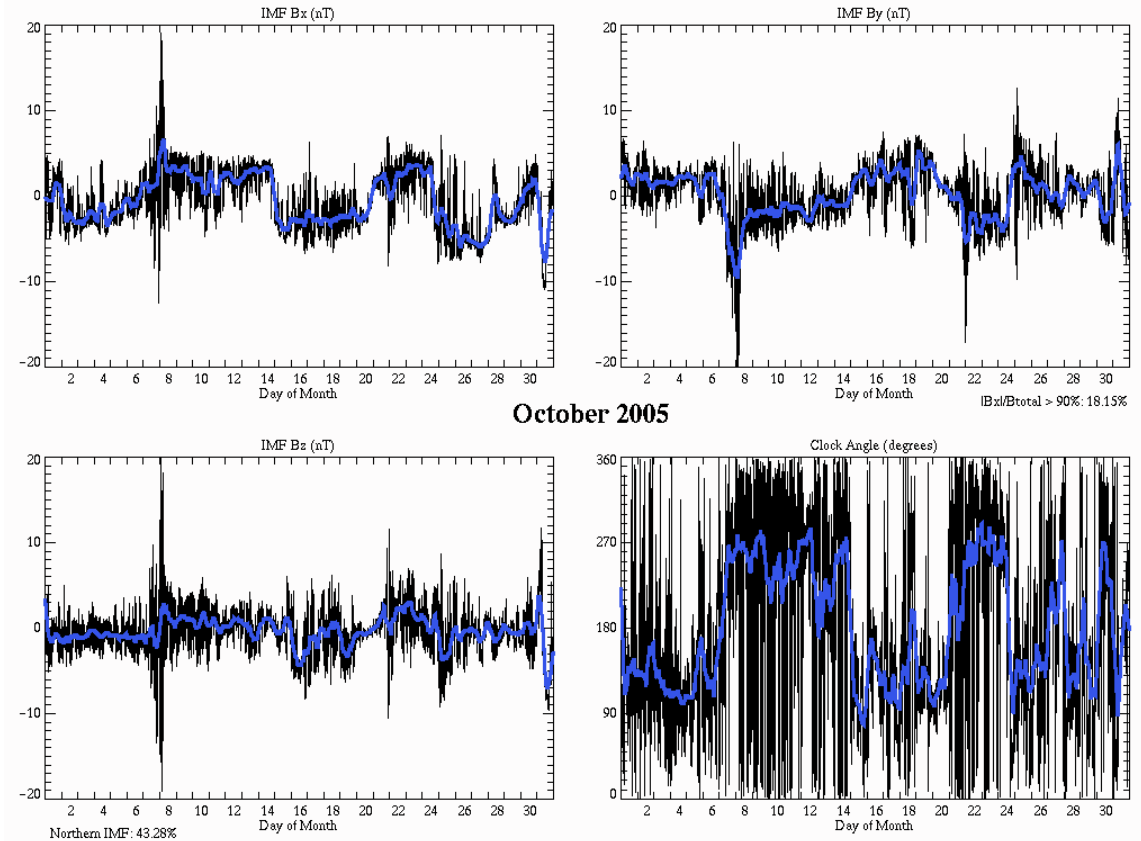


Figure 3.9 – ACE solar wind data for October 2005 showing IMF B_x , B_y , and B_z components as well as the IMF clock angle. The overlaid blue line shows a smoothed version of the data as a visual aid.

3.2.2 Solar Cycle Variations Using the Anti-parallel Model

From the results in the last section it seems that the IMF clock angle distribution is not significantly impacted by solar cycle variations. As a result, we expect that any variations using the anti-parallel model should be the results of: (1) variations in the magnitude of the IMF, (2) small differences in the IMF clock angle distributions, or (3) differences in the magnetospheric magnetic field as computed by the data-based T96 model. As is seen in Figure 3.10 below, although there are some small differences between solar maximum (left) and solar minimum (right), they are generally within a percent or two, which is not significant enough to be important.

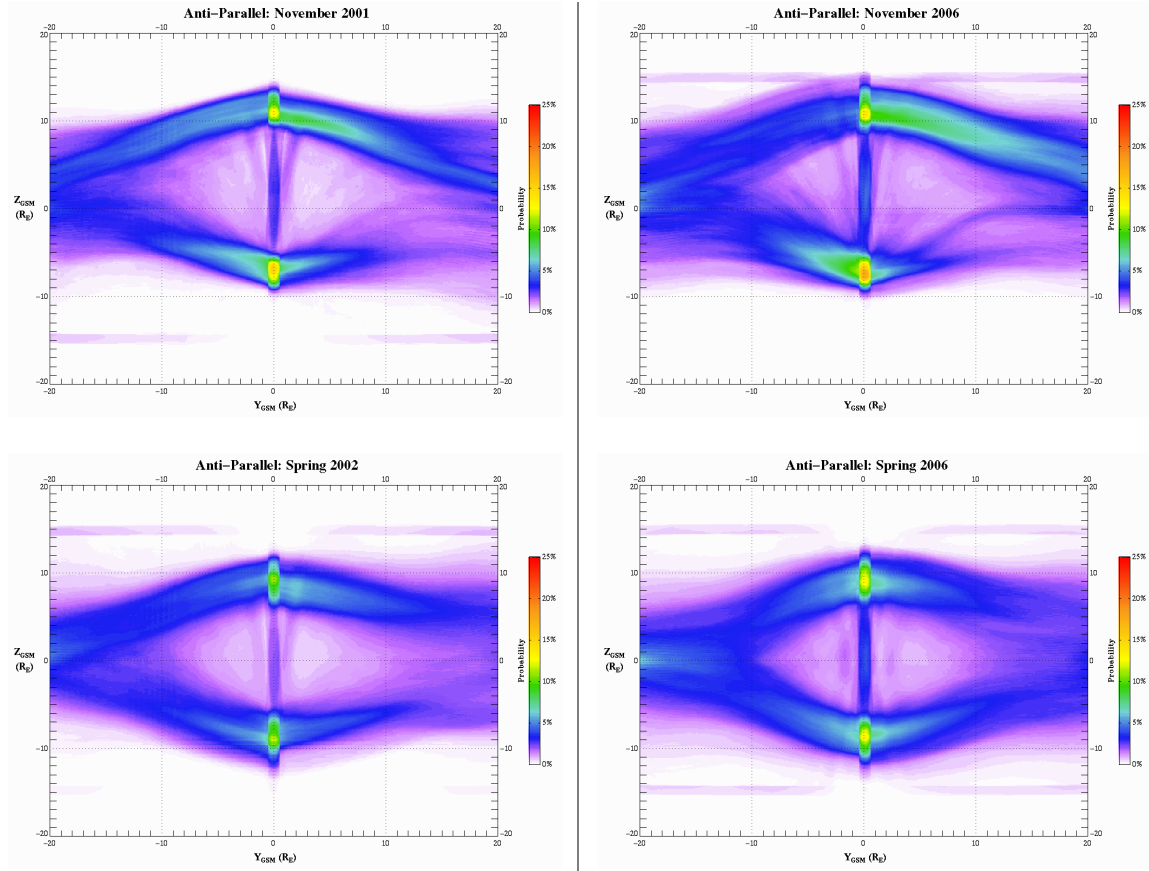


Figure 3.10 – Comparison of probability distributions at solar maximum (left) and near solar minimum (right) using the anti-parallel reconnection line model. The top two plots show probability distributions for the month of November, while the bottom plots show probability distributions for spring of 2002 and 2006.

3.2.3 Solar Cycle Variations Using the Trattner Model

From our analysis of the anti-parallel model, we expect that the Trattner model will also not exhibit any correlations to solar cycle based on the fact that the anti-parallel model and the Trattner model both take the same inputs. Indeed, except for some small variations, this is essentially what we see. There are some differences, but they are too small to be distinguishable from normal annual variations in the solar wind. In order to confirm or disprove these results, future studies should utilize additional data from other solar cycles.

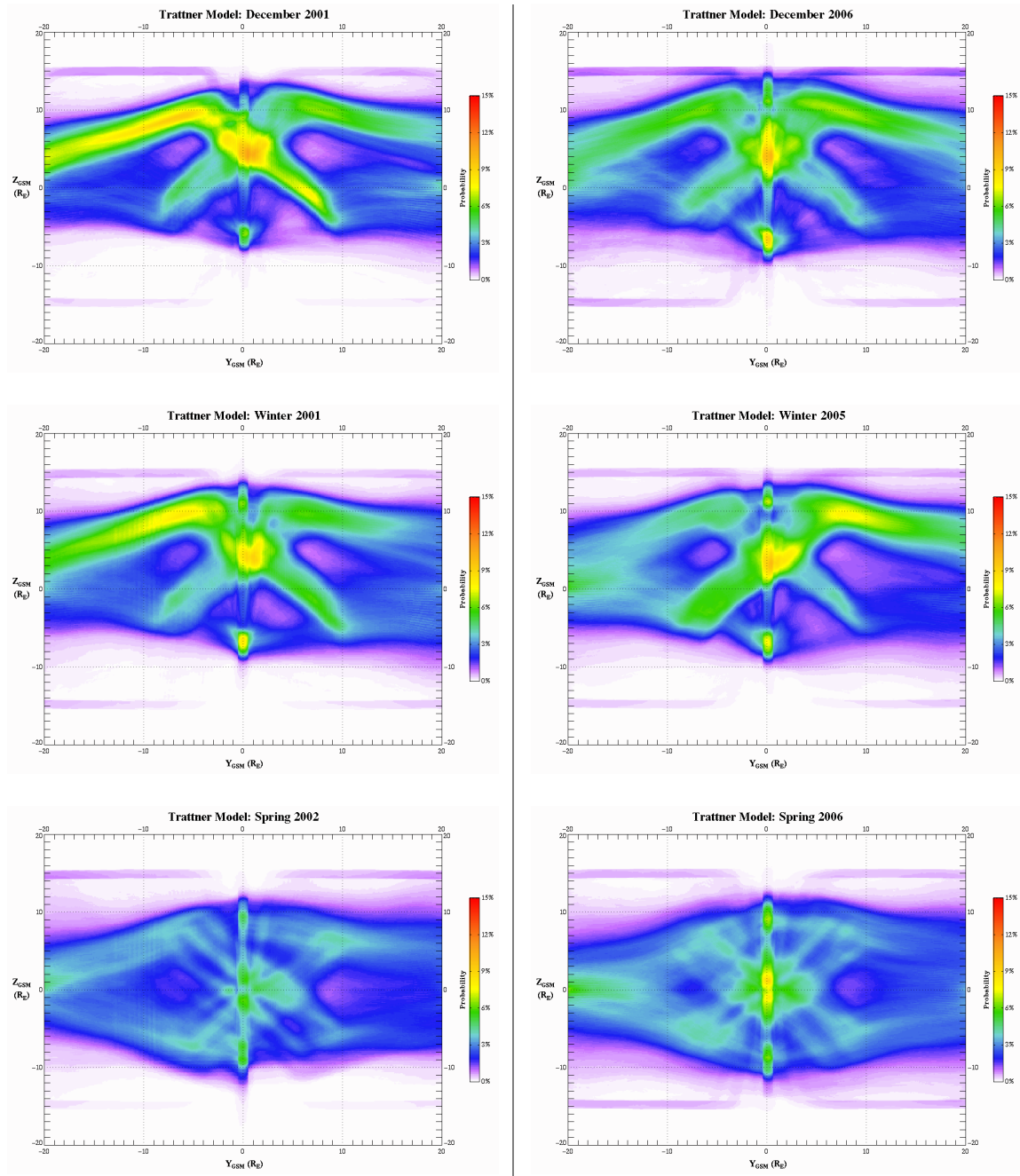


Figure 3.11 – Comparison of probability distributions at solar maximum (left) and near solar minimum (right) using the Trattner model. The top two plots show probability distributions for the month of December, the second row of plots show probability distributions for the winters of 2001 and 2005, and the bottom row shows probability distributions from spring 2002 and 2006.

4 Conclusions

In summary, we have confirmed our original hypothesis that there is a strong correlation between the distribution of reconnection lines across the dayside magnetopause and seasonal variation as a result of the Earth's dipole tilt and the solar wind sector distributions (due to the solar wind's Parker spiral structure). However, we have also seen that there is little or no connection between increased sunspot activity from the solar cycle and reconnection line distributions, which is a contrary result to our original expectations. Although the IMF direction and magnitude appear to be more random at solar maximum than they do at solar minimum, we showed that given a time scale of a month or more the average IMF appears to be approximately the same for both cases.

We also analyzed and compared three of the most popular reconnection line theories, including a simplified version of the tilted neutral line model, the anti-parallel model, and the recent Trattner model. Although the simplified version of the aging tilted neutral line model does not yield good results regarding the location of reconnection lines, we found good application for it as a tool for examining trends in IMF clock angles. Using this tool, we were able to discover that the average IMF for a given calendar segment appears to be the same from year to year, which is a rather unexpected result.

Our examinations using the anti-parallel model also yielded some interesting results, particularly in how the probabilities of locating a reconnection line at a particular location are spread across the magnetopause. The anti-parallel predicts that there are a few regions which you are much more likely to find a reconnection line passing through – specifically, the anti-parallel model predicts that most reconnection lines start at the cusps and follow a smooth path towards the ecliptic. The anti-parallel theory also

predicts that reconnection is less likely at the subsolar point than either of the other two models, although it does not predict a zero probability of reconnection at the subsolar point like you might expect from reading Crooker's original paper on anti-parallel reconnection line geometry. However, the anti-parallel model does predict a much lower probability of finding a reconnection line near the subsolar point, which is again at odds with the other two theories.

Although the Trattner model relies heavily on the anti-parallel model, the Trattner model yielded some strikingly different predictions than the anti-parallel model. While the anti-parallel model tends to generate reconnection line probability distributions which are partitioned between regions of high probability and regions of low probability, the Trattner model predicts a more evenly distributed probability distribution. However, it is important to realize that although the difference between a 2% probability and a 6% probability may seem small, in the latter case you are three times more likely to observe a reconnection line close by, which is a significant amount.

Along these same lines, the Trattner model also predicts that the high probability region near the subsolar point should shift northward and southward along with the Earth's dipole tilt. This is an important result because most other component reconnection theories (including the tilted neutral line) predict that reconnection can always occur at the subsolar point. Thus a space craft sent to look for reconnection at the subsolar point during the winter time may observe significantly fewer reconnection events at this location than predicted by older component reconnection theories.

There are many areas where this work could be improved or expanded. Although we tested our codes as rigorously as possible, there is always room for error, especially

since the codes total more than 100 pages in length. Moreover, additional data solar wind data is being made available in real time by ACE; additional solar wind data would prove especially invaluable in further studies of solar cycle trends. Also, as was briefly mentioned before, better methods of draping the IMF across the magnetopause are currently in development, and the reconnection line models are always being updated, revised, and reconsidered. Furthermore, new space craft such as NASA's Magnetospheric Multiscale (MMS) satellite cluster are currently being designed specifically for the purpose of investigating reconnection. Although MHD simulations have been very helpful in furthering our understanding of reconnection, there is no substitute for direct observation, and as more and better data becomes available we will see our understanding of reconnection continue to grow and flourish.

Bibliography

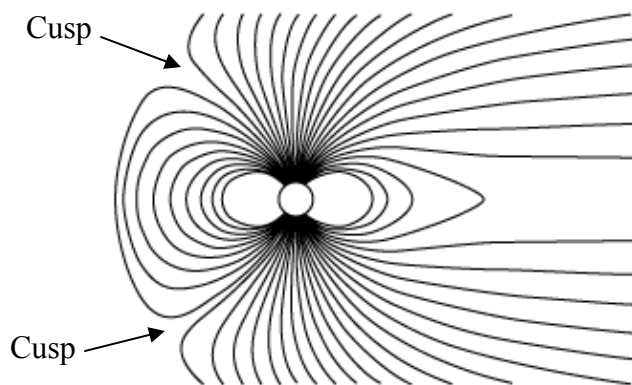
- Crooker, N. U. (1979). Dayside Merging and Cusp Geometry. *Journal of Geophysical Research* , 84, 951-959.
- Dungey, J. W. (1961). Interplanetary magnetic field and auroral zones. *Physical Review Letters* , 6, 47-48.
- Moore, T. E., Fok, M.-C., & Chandler, M. O. (2002). The dayside reconnection X line. *Journal of Geophysical Research* , 107.
- Phan et al. (2006). A magnetic reconnection X-line extending more than 390 Earth radii in the solar wind. *Nature* , 439, 175-178.
- Scurry, L., Russell, C. T., & Gosling, J. T. (1994). A statistical study of accelerated flow events at the dayside magnetopause. *Journal of Geophysical Research* , 99, 14815-14829.
- Sonnerup, B. U. Ö. (1970). Magnetic-field re-connexion in a highly conducting incompressible fluid. *Journal of Plasma Physics* , 4, 161-174.
- Trattner, K. J., Mulcock, J. S., Petrinec, S. M., & Fuselier, S. A. (2007). Location of the reconnection line at the magnetopause during southward IMF conditions. *Geophysical Research Letters* , 34.
- Trattner, K. J., Mulcock, J. S., Petrinec, S. M., & Fuselier, S. A. (2007). Probing the boundary between antiparallel and component reconnection during southward interplanetary magnetic field conditions. *Journal of Geophysical Research* , 112.
- Tysganenko, N. A. (1995). Modeling the Earth's magnetospheric magnetic field confined within a realistic magnetopause. *Journal of Geophysical Research* , 100, 5599-5612.

Glossary

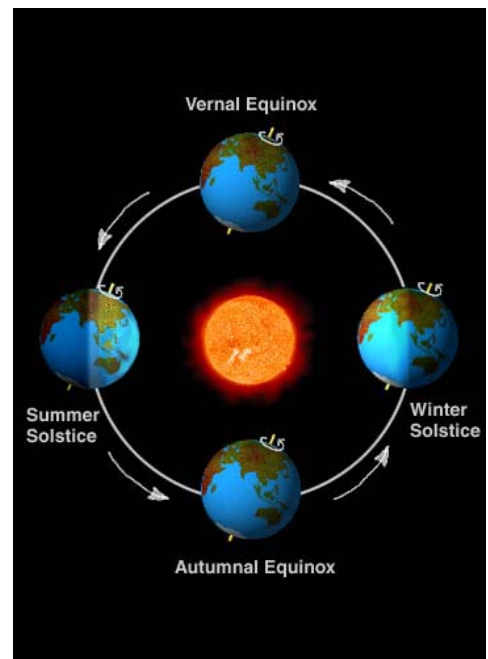
Clock Angle – the angle made by the IMF in the Y-Z GSM plane, as measured from the

ZGSM axis. $\text{Clock Angle} = \arctan\left(\frac{B_y}{B_z}\right)$

Cusps – often called polar cusps, these are “holes” in the magnetopause caused by the geometry of the Earth’s magnetic field. The cusps also allow direct access to the ionosphere, which is the layer of atmosphere beneath the magnetosphere.



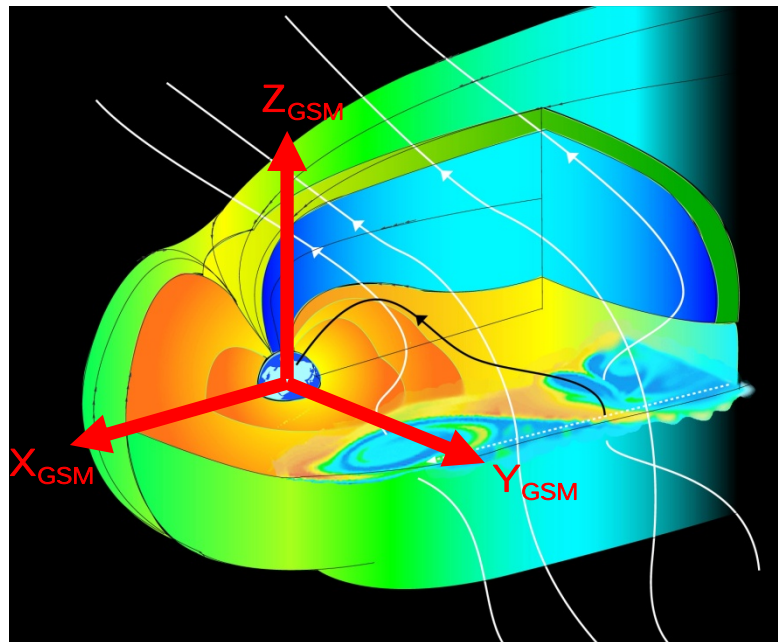
Dipole Tilt – the Earth’s magnetic field closely approximates a dipole. This dipole defines an axis, which is not necessarily aligned with the geographic poles. Furthermore, the Earth’s magnetic dipole seasonally tilts back and forth with respect to the Sun. The Earth’s magnetic dipole is used in defining the Z_{GSM} axis.



Dynamic Pressure – the dynamic pressure refers to the force of the solar wind exerts across the magnetopause surface. It is given by the equation $p_{dyn} = \frac{1}{2}\rho v^2$, where p_{dyn} is the dynamic pressure, ρ is the solar wind density, and v is the solar wind velocity.

Ecliptic Plane – the ecliptic plane is the plane in which the Earth orbits about the Sun. In GSM coordinates, it is the X-Y plane.

GSM Coordinates – GSM stands for “Geocentric Solar Magnetospheric.” The X-axis is aligned along the line between the Earth and the Sun, the Z-axis lies in the plane made by the X-axis and the Earth’s magnetic dipole axis so that the two axes are perpendicular, and the Y-axis is chosen so that the coordinate system is orthogonal and right-handed.



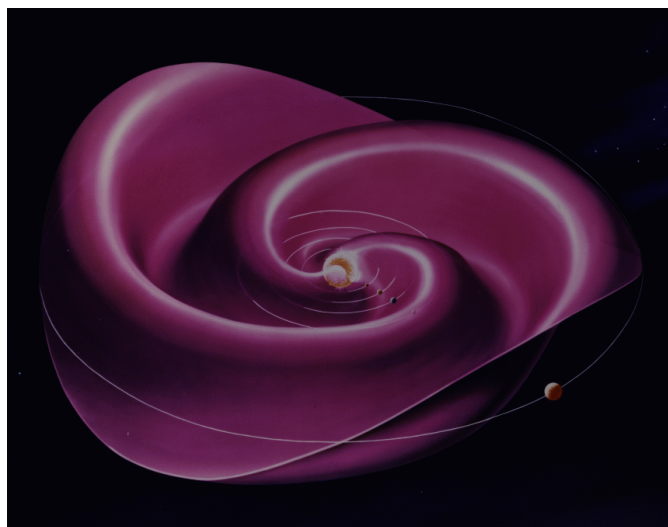
Interplanetary Magnetic Field (IMF) – the IMF is the magnetic field which is “frozen-in” to the solar wind via $\mathbf{E} \times \mathbf{B}$ drift. This rather counter-intuitive result comes from the solution of the MHD (magnetohydrodynamic) equations. The IMF can merge with the Earth’s magnetic field via magnetic reconnection.

Magnetic Shear Angle – the magnetic shear angle is simply the angle made between the IMF and the magnetospheric magnetic field at a particular point, as computed from a dot product. The magnetic shear is computed at each point on the magnetopause so that the magnetic shears form a scalar field.

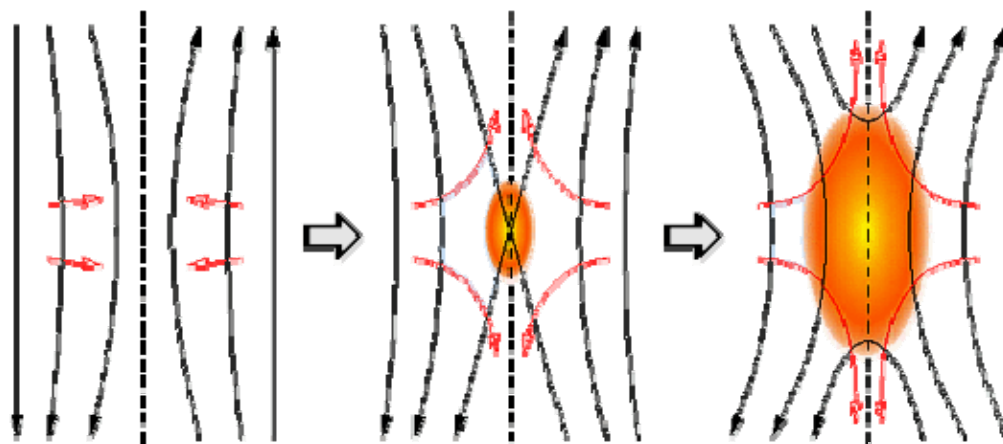
Magnetopause – the magnetopause is the boundary between the Earth's magnetic field and the continuous stream of solar wind emitted from the Sun. The size of the magnetopause fluctuates rapidly in response to variations in the dynamic pressure. The magnetopause is also where the IMF merges with the Earth's magnetic field via reconnection.

Magnetosphere – the magnetosphere is the outer-most layer of the Earth's atmosphere. It extends approximately $10 R_E$ (Earth radii) towards the Sun and more than $100 R_E$ (perhaps as much as $1000 R_E$) away from the Sun.

Parker Spiral – the Parker spiral represents the shape of the Sun's magnetic field as it is propagated throughout the solar system by the solar wind. The spiral shape is the result of the Sun's 27-day rotation. The Parker spiral is often described as a “ballerina skirt.”



Reconnection – magnetic reconnection is the process by which long magnetic field lines can merge with each other to form shorter field lines and thereby release large amounts of energy. The magnetic field lines are carried by plasma via $\mathbf{E} \times \mathbf{B}$ drift until the field lines cross each other, forming what is called an “X line” for obvious reasons. The center of the X is called the diffusion region, and is the point where the field lines break apart and then merge with the other field. The reconnected field lines then retreat rapidly from the diffusion region at the Alfvén velocity, sweeping plasma particles along with them. Although the field lines cannot be observed directly, the bidirectional jet of particles emitted from the diffusion region is a tell-tale reconnection signature. It is very important to note that the incoming magnetic field lines must be of opposite polarity (anti-parallel) in order for reconnected field lines to be correctly oriented. See [Sonnerup, 1970] for more technical details.



Reconnection Line – satellite observations indicate that reconnection diffusion regions form long, thin lines [Phan *et al.*, 2006] which extends across the entire magnetopause. The reconnection X line lies in the plane generated by the tangent vector of the reconnection line.

